Journal Pre-proofs

Research paper

Development of a multiparticulate drug delivery system for *in situ* amorphisation

Tobias Palle Holm, Marcel Kokott, Matthias Manne Knopp, Ben J. Boyd, Ragna Berthelsen, Julian Quodbach, Korbinian Löbmann

PII: S0939-6411(22)00216-8
DOI: https://doi.org/10.1016/j.ejpb.2022.09.021
Reference: EJPB 13860

To appear in: *European Journal of Pharmaceutics and Biopharmaceutics*

Received Date: 22 July 2022
Revised Date: 20 September 2022
Accepted Date: 24 September 2022

Please cite this article as: T. Palle Holm, M. Kokott, M. Manne Knopp, B.J. Boyd, R. Berthelsen, J. Quodbach, K. Löbmann, Development of a multiparticulate drug delivery system for *in situ* amorphisation, *European Journal of Pharmaceutics and Biopharmaceutics* (2022), doi: https://doi.org/10.1016/j.ejpb.2022.09.021

Development of a multiparticulate drug delivery system for *in situ* amorphisation

Tobias Palle Holm[1], Marcel Kokott[2], Matthias Manne Knopp[3], Ben J. Boyd[1], Ragna Berthelsen[1], Julian Quodbach[2,4] and Korbinian Löbmann[1*]

[1] Department of Pharmacy, Faculty of Health and Medical Sciences, University of Copenhagen, Copenhagen, Denmark

[2] Institut für Pharmaceutische Technologie Und Biopharmacie, Heinrich-Heine-Universität, Düsseldorf, Germany

[3] Bioneer:FARMA, Department of Pharmacy, Copenhagen, Denmark

[4] Department of Pharmaceutics, Utrecht Institute for Pharmaceutical Sciences, Utrecht University, Utrecht, The Netherlands

[*] Corresponding author: **korbinian.loebmann@sund.ku.dk;** Phone +45 35 32 05 41

Keywords: *in situ* amorphisation, amorphous solid dispersion, microwave irradiation, celecoxib, sodium dihydrogen phosphate, multiparticulate drug delivery system

Abstract

In the current study, the concept of multiparticulate drug delivery systems (MDDS) was applied to tablets intended for the amorphisation of supersaturated granular ASDs *in situ,* i.e. amorphisation by microwave irradiation within the final dosage form. The MDDS concept was hypothesised to ensure geometric and structural stability of the dosage form and to improve the *in vitro* disintegration and dissolution characteristics. Granules were prepared in two sizes (small and large) containing the crystalline drug celecoxib (CCX) and polyvinylpyrrolidone/vinyl acetate copolymer (PVP/VA) at a 50 % w/w drug load as well as sodium dihydrogen phosphate monohydrate as the microwave absorbing excipient. The granules were subsequently embedded in an extra-granular tablet phase composed of either the filler microcrystalline cellulose (MCC) or mannitol (MAN), as well as the disintegrant crospovidone and the lubricant magnesium stearate. The tensile strength and disintegration time were investigated prior to and after 10 min of microwave irradiation (800 and 1000 W) and the formed ASDs were characterised by X-ray powder diffraction and modulated differential scanning calorimetry. Additionally, the internal structure was elucidated by X-ray micro-Computed Tomography (XμCT) and, finally, the dissolution performance of selected tablets was investigated. The MDDS tablets displayed no geometrical changes after microwave irradiation, however, the tensile strength and disintegration time increased. Complete amorphisation of CCX was achieved only for the MCC-based tablets at a power input of 1000 W, while MAN-based tablets displayed partial amorphisation independent of power input. The complete amorphisation of CCX was associated with the fusion of individual ASD granules within the tablets, which impacted the subsequent disintegration and dissolution performance. For these tablets, supersaturation was only observed after 60 min. On the other hand, the partially amorphised MDDS tablets displayed complete disintegration during the dissolution experiments, resulting in a fast onset of supersaturation within 5 min and an approx. 3.5-fold degree of supersaturation within the experimental timeframe (3 h). Overall, the MDDS concept was shown to potentially be a feasible dosage form for *in situ* amorphisation, however, there is still room for improvement to obtain a fully amorphous and disintegrating system.

Keywords: *in situ* amorphisation; amorphous solid dispersion; microwave irradiation; multiparticulate drug delivery system; compaction; celecoxib; polyvinylpyrrolidone; sodium dihydrogen phosphate

1. Introduction

For decades, the pharmaceutical drug discovery pipeline has been challenged by poorly water-soluble small molecules which are currently estimated to make up 80-90 % of all drugs in development [1-4]. A prerequisite for oral bioavailability is getting and sustaining the drug in solution, as only dissolved drug can be absorbed from the gastrointestinal tract [5]. Oral administration is the most preferred route of administration for several reasons including patient compliance, manufacturing and cost-effectiveness. However, the poor water solubility of most drug candidates remains a considerable challenge in the development of oral drug delivery systems [6, 7].

A multitude of enabling formulation strategies have been proposed to deal with the low aqueous solubility and in turn low oral bioavailability [8, 9]. One way to address this challenge is to transform the physical form of the drug material – from the crystalline to the amorphous form. Whereas the molecular packing in crystalline form(s) has three-dimensional long-range order and is physically stable, the packing is disordered in the amorphous form and thus the molecules have an increased enthalpy as well as mobility. The loss of order in the material lowers the barrier for dissolution, resulting in increased apparent solubility and dissolution rate [6, 10, 11]. However, the high energy state comes with an inherent thermodynamically instability of the amorphous form, resulting in a driving force to revert to the parent crystalline form by relaxation, nucleation and recrystallisation and thus, the gain in solubility will inevitably be lost over time [11-13]. To increase the oral bioavailability based on the solubility and dissolution rate advantage of the amorphous form of a drug, it is thus necessary to stabilise the amorphous drug in a drug delivery system, typically by the addition of stabilising excipients.

Thus, dispersion of the amorphous drug in a polymeric matrix (i.e., amorphous solid dispersions, ASDs) is the most studied amorphous formulation approach for oral drug delivery [14, 15]. By incorporating the amorphous drug in a polymeric matrix (such as polyvinylpyrrolidone/vinyl acetate (PVP/VA) or hydroxypropyl methylcellulose), the mobility of the drug molecules is greatly reduced by the antiplasticising effect of the polymer and results in kinetic stabilisation of the amorphous drug [15, 16]. To ensure thermodynamic stability and extended shelf-life of an ASD, it is necessary to keep the drug load below the solubility of the drug in the given polymer [15, 17, 18]. However, the relatively low saturation solubility of many small molecule drugs in

commercial pharmaceutical polymers increases the amount of polymer required to accommodate the therapeutic dose and hence, induces practical challenges from a dosage form size perspective [14-16, 19, 20].

Polymer-based ASDs are usually prepared by hot-melt extrusion or spray drying, followed by further downstream processing of the ASD into a final dosage form [14, 21, 22]. Additionally, the high polymer content in most ASDs negatively impacts the compactability and the subsequent disintegration behaviour, requiring increased amounts of excipients (filler and disintegrant) to counter these effects [23, 24]. Downstream processing of ASDs, such as particle size reduction, mixing, granulation, compaction and coating, are also known to potentially induce crystallisation of the embedded amorphous drug [25-29].

An alternative to this traditional manufacturing pathway is the generation of the amorphous form of the drug in the final dosage form immediately before administration through the application of some *in situ* stimulus [30-32]. With this approach, potential recrystallisation as a result of downstream processing is greatly reduced due to the short time between amorphisation and administration. Furthermore, this concept aims to circumvent stability issues of ASDs with drug loadings above the saturation solubility of the drug in a given polymer. This so-called "*in situ* amorphisation" can be achieved using microwave radiation [33-35]. Using this concept, heat is generated inside the final dosage form, which is the main driver for the amorphisation process and the formation of the ASD. Microwave heating relies on the presence of dipolar molecules that are coupling with the oscillating electromagnetic field applied in the microwave cavity, resulting in the generation of heat by friction (dielectric heating) [36, 37]. Most drugs, and the commonly utilised pharmaceutical excipients, do not display dielectric properties. Hence, they are not directly responding to microwave heating, which makes it necessary to add additional excipients with intrinsic dielectric properties to achieve amorphisation *in situ* [38, 39]. By using absorbed water as the primary excipient with dielectric properties (at the common frequency of 2.45 GHz [40, 41]), partial *in situ* amorphisation of the drug celecoxib (CCX) in polyvinylpyrrolidone was reported by Edinger *et al.* in 2018 [34] and complete amorphisation was reported by Hempel *et al.* in 2020 [35]. However, the drug loading in the polymer was only 20-30 % w/w in the studies by Edinger *et al.*[34] and Hempel *et al.*[35], and still well below the saturation solubility of approx. 40 % w/w at ambient temperature [42]. By using polyethylene glycol (PEG) as a dielectric excipient, Hempel *et al.* [43] achieved a 50 % w/w CCX load in a combined PEG-PVP polymeric matrix and an approx. 1.25-fold supersaturation.

Recent work by the authors has suggested that the addition of crystalline hydrates that dehydrate upon microwave processing, and hence provide an on-demand dielectric heating source throughout the dosage form, allows for complete *in situ* amorphisation [44]. Additionally, this concept allowed the preparation of highly supersaturated ASDs by microwave irradiation, with drug loadings up to 90 % w/w corresponding to 2.3 to 10-fold supersaturation, by incorporating sodium dihydrogen phosphate monohydrate (NaH_2PO_4 monohydrate) in the dosage form [45]. Whilst *in situ* amorphisation could be successfully realised on compacts comprising only the drug, polymer and inorganic salt hydrate, these compacts did not present a final dosage form. The main challenges with *in situ* amorphisation, in general, were the ability to retain the shape of the compacts at increased temperature and humidity and to achieve sufficient disintegration of the resulting monolithic ASDs. As a result of the microwave processing, the initial individual drug and polymer particles fused to form large monolithic ASDs which in turn hampered the disintegration and reduced the overall dissolution performance [33, 45, 46].

This work aimed to investigate the possibility of preparing a final solid dosage form, feasible for *in situ* amorphisation by microwave irradiation, based on the principle of a multiparticulate drug delivery system (MDDS) [47]. In the current study, NaH_2PO_4 monohydrate was utilised as the source of dielectric material and combined in granules with CCX as the model drug and a relevant vinyl polymer (PVP/VA). The manufactured granules were then embedded in tablets with a filler-binder (microcrystalline cellulose, MCC, or mannitol, MAN) and a superdisintegrant (crospovidone). The hypothesis was that the MDDS approach could potentially address the previously identified shortcomings associated with microwave-induced *in situ* amorphisation; i) physical form stability, ii) mechanical strength and disintegration behaviour, and iii) drug release from the final dosage form. Along with the two filler-binders, MCC and MAN, two granule size fractions (d(5.0) 358. ± 35.0 and 635.9 ±14.2 μm, denoted *small and large*), five compaction pressures (50-250 MPa) as well as two microwave power inputs (800 and 1000 W at 2.45 GHz, for 10 min) were investigated to study the effect on the mechanical strength, disintegration behaviour, the form stability and internal tablet structure, as well as amorphisation of the drug load. Finally, the dissolution behaviour of the most promising formulations was investigated to assess the possible solubility and dissolution rate advantage.

2. Material and methods

2.1 Materials

Celecoxib (CCX) was purchased from Fagron (Rotterdam, Netherlands). Polyvinylpyrrolidone/vinyl acetate (PVP/VA, Kollidon® VA64, Mw = 45,000-70,000 g/mol) was kindly gifted from BASF (Ludwigshafen, Germany) and sodium dihydrogen phosphate (NaH_2PO_4) mono- and anhydrate were kindly gifted by Merck (Darmstadt, Germany). Microcrystalline cellulose (VivaPur 102, MCC) and mannitol (Pearlitol 200 SD, MAN) were purchased from JRS Pharma (Patterson, NY, USA) and Roquette (Lestrem, France), respectively. Crospovidone (Kollidon® CL) was purchased from BASF (Ludwigshafen, Germany), magnesium stearate (MgSt) from UNIKEM (Copenhagen, Denmark) and Vcaps Plus capsules (HPMC, size 00) were kindly gifted by Lonza (Strasbourg, France). Fasted state simulated intestinal fluid (FaSSIF) powder was purchased from Biorelevant Ltd. (London, United Kingdom). Sodium chloride and sodium hydroxide were purchased from Merck (Darmstadt, Germany). Methanol (≥99.8%, analytical HPLC grade) was purchased from VWR International Ltd. (Poole, United Kingdom). Purified water was freshly prepared using a MilliQ system from ELGA LabWater (High Wycombe, United Kingdom).

2.2 Preparation of granules

Prior to granulation, the drug and excipients were sieved (<71 µm) and a physical mixture of CCX (37.5 % w/w), PVP/VA (37.5 % w/w) and NaH_2PO_4 monohydrate (25 % w/w) were prepared by mixing for 8 min at 45 rpm in an AR 400 cube mixer by Erweka (Langen, Germany).

Dry granulation of the physical mixture was performed on a TFC-LAB Micro roller compactor by Freund-Vector Corporation (Marion, Iowa, USA). The roller compactor was equipped with ribbed rim rollers (50 mm diameter, 14 mm effective width) and operated at 1.5 mm gap width, 0.8 rpm roll speed, with 41.4 bar pressure on the rollers and 10 rpm screw speed in the hopper. The resulting ribbons were milled with a 1.0 mm rasp sieve with a TFC-Micro granulator by Freund-Vector Corporation (Marion, Iowa, USA). The final granules were split into two fractions by sieving (i.e. 355-500 μm and 500-710 µm), in the following denoted *small* and *large*.

149 *2.2.1 Particle size determination*

150 After dry granulation, the particle size distribution of the two granule fractions was analysed by laser diffraction,
151 using a Malvern Mastersizer 2000 with a dry powder Scirocco 2000 stage from Malvern Panalytical LTD
152 (Malvern, UK). Approximately 2 g of the granular samples were placed in the sample feeder and the
153 measurements were conducted using a pressure of 0.7 bar and with a feed rate of 40 %, to ensure preservation
154 as well as separation of the granules. The analysis was performed in triplicate and the results are reported as
155 the mean particle size (d0.5 [µm] ± SD).

156 **2.3 Preparation of tablets**

157 Powder mixtures of large or small granules (section 2.2) and the extragranular excipients: lubricant (MgSt),
158 filler (MCC or MAN) and superdisintegrant (crospovidone) were prepared as 50 % w/w ASD granules (18.75
159 % w/w of both CCX and PVP/VA, 12.5 % w/w NaH_2PO_4 monohydrate), 39 % w/w filler, 10 % w/w crospovidone
160 and 1 % w/w MgSt. Four powder mixtures, with combinations of all granule sizes (large and small) and fillers
161 (MCC and MAN), were prepared. The filler materials and disintegrant were used as received, while MgSt was
162 sieved (<125 μm) before weighing and mixing. The mixing process was conducted in two steps; In the first
163 step, the granules, filler and disintegrant were mixed for 10 min (101 rpm), and in the second step 1 % w/w
164 MgSt was added and the mixing was continued for an additional 2 min (101 rpm) in a T2F Turbula Mixer by
165 Willy A. Bachofen (Basel, Switzerland). Tablets of approx. 200 mg were compressed with 8 mm flat-faced
166 punches at varying compaction pressures (from 50 to 250 MPa in increments of 50 MPa) using a STYL'One
167 Evo compaction simulator equipped with a force feeder from Medel'Pharm (Beynost, France). The
168 manufacturing was conducted at 21 °C and 45% RH and the MDDS tablets were subsequently stored airtight
169 at ambient temperature before further analysis and microwave irradiation.

170 **2.4 Tablet characterisation**

171 *2.4.1 Tensile strength*

172 The tensile strength of the prepared MDDS tablets (section 2.3) was determined prior to and after microwave
173 irradiation. A SmartTest 50 from SOTAX s.r.o. (Prague, Czech Republic) was used to measure the breaking

force, diameter, height and mass of the MDDS tablets. Subsequently, the tensile strength [MPa] was calculated as per equation 1 [48] and reported as mean +/- SD (n=10).

Equation 1 $$tensile\ strength = \frac{2F}{\pi * h * d}$$

F = breaking force [N], h = height [mm] and d = diameter [mm].

2.4.2 Disintegration

Disintegration testing was performed using a PTZ 2E disintegration apparatus from Pharma Test (Hainburg, Germany) and in accordance with Ph. Eur 2.9.1 (10.7, October 2021) for uncoated tablets. The disintegration tests were carried out in demineralised water (37.0 ± 2 °C) and reported as mean +/- SD (n=6).

2.5 *In situ* amorphisation by microwave irradiation

A dual magnetron Microwave 3000 oven from Anton Paar GmbH (Graz, Austria), operating at a frequency of 2.45 GHz, was used for microwave irradiation of the MDDS tablets. The tablets were loaded in individual Vcaps Plus HPMC capsules (size 00) to imitate a blister pack where tablets are confined individually. The capsule-enclosed tablets were subsequently sealed in separate 5 mL microwave transparent polypropylene Eppendorf tubes, distributed in a 64-slot rotating (3 rpm) sample assembly to limit conductive heating and microwave irradiated at a power output of 1000 W for 10 min. To avoid damage to the magnetrons through the reflection of radiation, 16 vials containing 1.5 mL purified water were additionally positioned in separate wells in the rotating sample assembly.

2.6 Solid state analysis

The MDDS tablets were subjected to solid-state analysis after microwave irradiation. X-ray powder diffraction (XRPD) was used to assess the residual CCX crystallinity and the dehydration of NaH_2PO_4 monohydrate after microwave irradiation. Modulated differential scanning calorimetry (mDSC) was used to investigate the homogeneity of the embedded ASDs.

2.6.2 X-Ray Powder Diffraction (XRPD)

Prior to analysis, the MDDS tablets were gently ground and samples were placed on aluminium sample plates and flattened to a fixed height. An X'Pert PRO X-ray powder diffractometer from PANalytical (Almelo, The

Netherlands), equipped with a PIXcel detector, was used to collect diffractograms. The diffractograms were collected from angles 4-36 °2θ with a scan speed of 0.067 °2θ/s and a step size of 0.026 °2θ, using a reflection spinner X-ray stage and a CuKα radiation source (45 KV, 40 mA, λ=1.54187 Å). Data collection and analysis were performed using, respectively, the X'Pert Data Collector software (version 2.2i) and X'Pert HighScore Plus software (version 2.2.4) from PANalytical (Almelo, The Netherlands)-.

2.6.3 Modulated differential scanning calorimetry (mDSC)

The T_g, phase behaviour, and residual CCX crystallinity in MDDS tablets after microwave irradiation was investigated using a Discovery DSC from TA-Instruments-Waters LCC (New Castle, DE, United States). The instrument was calibrated using an indium standard and measurements were performed under a 50 mL/min nitrogen purge. The MDDS tablets were gently ground and loaded in Tzero aluminium pans with Tzero aluminium hermetic lids at a sample size of 9-12 mg. The samples were cooled to -20 °C, kept isothermal for 2 min and scanned to 180 °C at a rate of 3 °C/min, and applied a modulation amplitude of 1 °C and a 50 s period. The T_g was determined as the half-height of the step-change in the reversing heat flow signal, using the Trios software (version 4.5.0) from TA-Instruments-Waters LCC (New Castle, DE, USA).

2.7 X-ray micro-Computed Tomography (XμCT)

The internal structure of the MDDS tablets, prior to and after microwave irradiation, was analysed by XμCT. MDDS tablets were mounted at a 20-40° angle and recorded during a 360° rotation by a CT-ALPHA from ProCon X-ray (Sarstedt, Germany) with a voxel resolution of 6 µm (1888 × 1888 × 1505 voxels). The imaging was performed with an applied voltage of 100 kV and an amperage of 100 µA on the X-ray source. Reconstruction of the raw images was performed in VGStudio 3.0.1 by Volume Graphics GmbH (Heidelberg, Germany) and final visualisation of the .tiff image stack was performed in 3DSlicer [49].

2.8 Dissolution

A USP type II DT70 dissolution tester from ERWEKA GmbH (Heusenstamm, Germany) was used to assess the dissolution performance of selected MDDS tablets prior to and after microwave irradiation. Dissolution testing was performed in 250 mL mini-USP dissolution vessels containing 50.0 mL FaSSIF (prepared according to the manufacturer's instructions, Biorelevant Ltd. (London, United Kingdom)) at 37.5°C, with

MDDS tablets corresponding to a relevant clinical CCX dose (3 tablets, approx. 110 mg CCX[50-52]) and mini-paddles operated at 150 rpm. At specified time points (0, 1, 5, 10, 15, 20, 30, 45, 60, 90, 120, and 180 min), aliquots of 0.5 mL were withdrawn and centrifuged for 5 min at 12,000 x g in an ESPRESSO Centrifuge from Thermo Fisher Scientific Instruments Co., Ltd. (Shanghai, China). After centrifugation, the supernatant was diluted in methanol and analysed by HPLC-UV (section 2.8.1).

Additionally, an *in vivo* relevant dissolution setup, displaying non-sink conditions using a 50 mL dissolution volume and a clinically relevant dose of approx. 110 mg CCX, was selected to allow evaluation of the possible supersaturating effect of the prepared ASDs [53, 54]. The dissolution experiments were performed in triplicate (n=3).

2.8.1 Quantification of celecoxib

CCX was quantified by high-performance liquid chromatography (HPLC) coupled to ultraviolet (UV) detection using an Agilent 1260 Infinity chromatographic system, with an Agilent 1290 Diode Array Detector from Agilent Technologies (Santa Clara, USA). The mobile phase of methanol and purified water in a 75:25 % v/v ratio was pumped through an ACE C18-PFP column (100 × 4.6 mm, 5 µm) from Advanced Chromatography Technologies Ltd. (Aberdeen, Scotland) at a flow rate of 1.0 mL/min and a temperature of 40 °C. The concentration of CCX in the samples was quantified as the area under the curve (AUC) of the UV absorbance peak at a wavelength of 251 nm, after a 10 µL sample injection. The CCX standard curve was linear in the range of 0.8–80 µg/mL ($R^2 > 0.99$).

3. Results and Discussion

3.1 Tablet characteristics before microwave irradiation

The tabletability of the proposed MDDS formulations, i.e., the correlation of the compaction pressure with the tensile strength of the resulting tablets, was investigated to assess the suitability of the proposed formulations from a manufacturing perspective and to determine an acceptable range of compaction pressures. As a function of filler material and granule fraction, the tabletability of the formulations was investigated with a range of compaction pressures appropriate for traditional tablet manufacturing (50-250 MPa), and the results are displayed in Figure 1a.

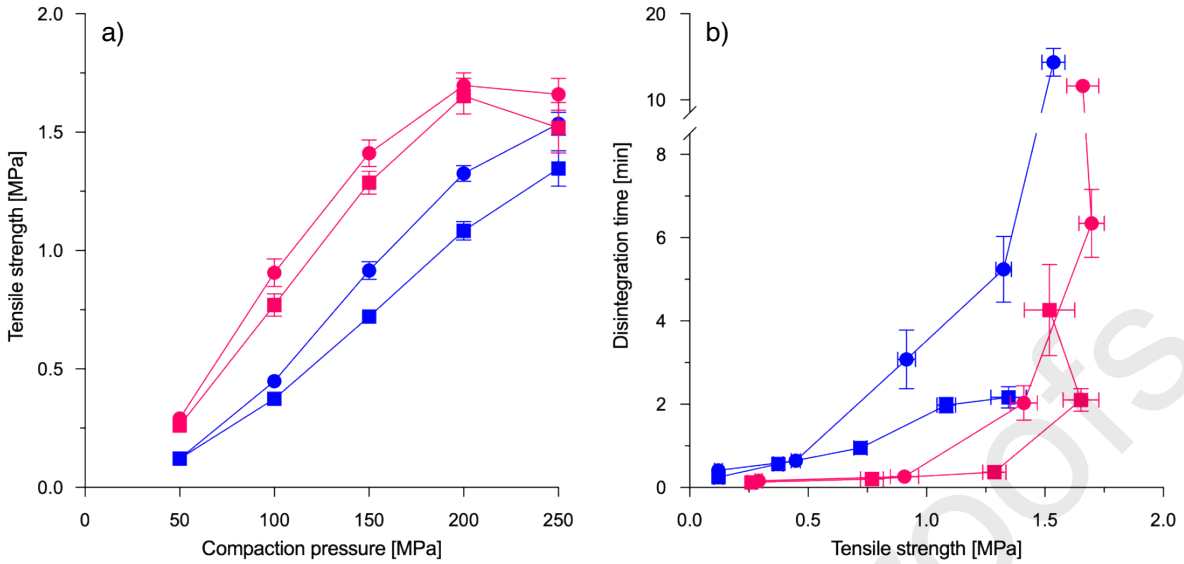

Figure 1 a) Tabletability of MDDS formulations prior to microwave irradiation, b) Disintegration time of MDDS tablets prior to microwave irradiation as a function of tensile strength. Tablets based on MCC (pink) and MAN (blue), with granule sizes large (square) and small (circle). Mean +/- SD (tensile strength, n=10; disintegration time, n=6).

Overall, an increasing tensile strength was observed with increasing compaction pressure across all the investigated formulations (Figure 1a). The MDDS tablets with MCC as the filler displayed a higher absolute tensile strength compared to the MDDS tablets prepared with MAN as the filler, at all the investigated compaction pressures besides 250 MPa (Figure 1a). A maximum tensile strength of 1.7 ± 0.1 and 1.5 ± 0.1 MPa was recorded for tablets based on MCC and MAN, respectively. Considering further handling and downstream processing, a suitable tensile strength of 1-2 MPa has been proposed [55]. Independent of the filler material, a consistent increase in tensile strength of the tablets was also observed with a decreasing ASD granule size at compaction pressures ≥100 MPa, but the trend was more pronounced in tablets based on MAN. The increase in tensile strength is hypothesised to be a combined effect of the increase in available surface area for binding with decreasing granule size, along with the individual compaction behaviour of MAN and MCC [56]. By increasing the compaction pressure from 200 to 250 MPa for the tablets based on MCC, the tensile strength was found to reach a plateau or decrease, indicating an upper threshold for the tensile strength, as a result of a more pronounced elastic deformation, and associated recovery, for the filler at high compaction pressures. On the other hand, the tablets with MAN as the filler displayed an increasing tensile strength with increasing compaction pressure throughout the investigated range (Figure 1a). The initial results indicated the suitability of both MCC and MAN as fillers for the MDDS tablets over a wide range of compaction

pressures (100-250 MPa), allowing normal handling as well as further downstream processing prior to microwave irradiation.

As the applied compaction pressure during tabletting is known to affect the resulting tablet porosity and influence the overall disintegration behaviour, the disintegration time was subsequently investigated prior to microwave irradiation and displayed as a function of the experimentally determined tensile strength in Figure 1b. The disintegration time for the investigated MDDS tablets prior to microwave irradiation was observed from 12 sec to approx. 15 minutes, fulfilling the Ph.Eur. (10.7, October 2021) specifications for uncoated tablets (<15 min), and with a low sample variation across formulation and manufacturing variables. Tablets with MCC as the filler displayed overall faster disintegration times, at an equivalent tensile strength in the 0.5-1.5 MPa range, compared to MAN-based tablets (Figure 1b). An increasing disintegration time was observed with decreasing size of the embedded granules, with the tablets containing small granules showing a significantly increased disintegration time compared to the tablets based on large granules. At the recorded extremes of the tensile strength (< 0.5 and > 1.5 MPa), the effect on disintegration was a result of either a lack of mechanical strength due to a loss in interparticular bonding capacity or a markedly reduced porosity, respectively.

Based on the initial tabletability and the disintegration behaviour of the tablets prior to microwave irradiation (Figure 1a and b), further investigations were performed at three different compaction pressures for MAN and MCC-based tablets yielding comparable tensile strength (0.7-1.7 MPa), i.e. in the range of 150-250 and 100-200 MPa for MAN- and MCC-based tablets, respectively.

3.2 Tablet characteristics after microwave irradiation

The processing of polymeric systems by microwave radiation has previously been shown to cause fusion of the polymeric particles and the formation of a monolithic ASD in simple tablets comprising only the drug, polymer and dielectric excipients [33-35, 46]. Overall, this fusion of polymer has previously been shown to result in low porosity and high tablet hardness, ultimately leading to little or no disintegration of the monolithic ASD. This in turn led to a very slow drug release rate [33, 44, 46]. Based on these past observations, it was hypothesised that the microwave processing would also cause structural changes in the MDDS tablets due to the fusion of individual particles in the individual granules and potentially a fraction of the extragranular matrix - at least to some degree for extragranular particles in direct contact with the granules. Thus, the effect of

298 microwave irradiation at two power inputs (800 and 1000 W) on the form stability, tensile strength, and
299 disintegration behaviour of the selected MDDS tablets was investigated and the results are displayed in Figure
300 2 and Table 1.

301 The neat MDDS tablets displayed a white and uniform appearance prior to microwave irradiation, independent
302 of filler as well as the size of the embedded granules (Figure 2). The outline of the embedded granules was
303 barely visible on the surface of the investigated tablets. After microwave irradiation, the geometric shape of all
304 the investigated MDDS tablets was retained at both 800 and 1000 W power input, albeit with visible surface
305 changes (Figure 2). The MCC-based tablets displayed changes in the embedded granules, visible as
306 translucent areas within the otherwise opaque white extragranular phase after microwave irradiation at 800 W.
307 However, after microwave irradiation at 1000 W, large light yellow transparent areas, as well as increased
308 roughness, were observed on the surface of the MCC-based tablets, indicating the fusion of two or more
309 granules due to the size of the observed areas. Microwave irradiation of tablets based on MAN caused a visible
310 increase in surface roughness at 800 W and a further increase at 1000 W, with a simultaneously more
311 pronounced granule outline as well as translucence with increasing microwave power input (Figure 2). The
312 change in the visual appearance of the granules after microwave irradiation, from white to light yellow
313 translucent in the case of tablets based on MCC, indicated the formation of glassy matrices within the tablets.
314 The observed colour change in the MCC-based tablets after microwave irradiation at 1000 W is suggested to
315 be a combined result of the granule fusion and slight yellow colour of neat amorphous CCX. No chemical
316 degradation of CCX was reported upon microwave irradiation of a comparable drug-polymer system by Holm
317 *et al.* [45].

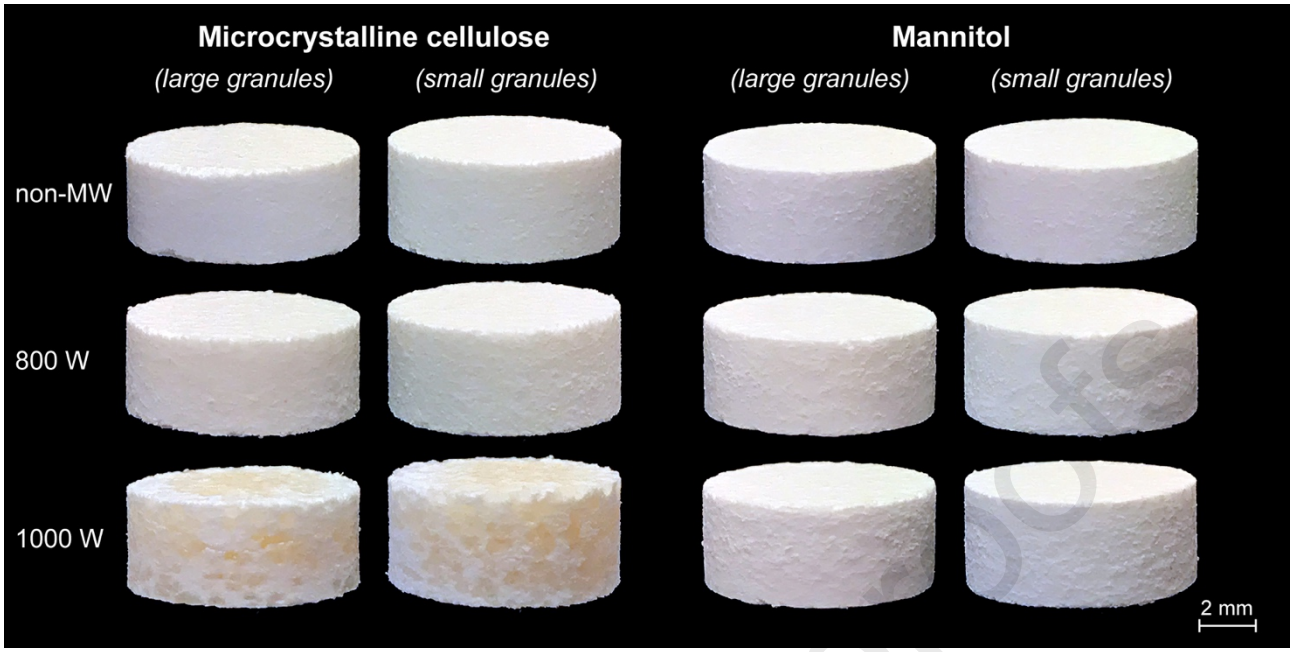

Figure 2 Visual evaluation of a selection of representative tablets (diameter = 8 mm) subjected to microwave irradiation at 800 and 1000 W at 2.45 GHz (10 min), as well as prior to microwave processing (non-MW). Tablets were prepared with different fillers, different granule particle sizes and different compaction pressures; microcrystalline cellulose large and small granules at 200 and 100 MPa, mannitol large and small granules at 250 and 150 MPa, respectively.

The tensile strengths of the tablets were 0.4-3.7 MPa, accounting for either a decrease or increase after microwave irradiation depending on the changes in the internal structure (see section 3.3). The microwave irradiated tablets based on MCC generally displayed a higher tensile strength compared to tablets based on MAN, with a comparable tensile strength after microwave irradiation at 800 W and a significantly increased strength at 1000 W power input (Table 1). Most of the investigated tablets based on MAN showed reduced tensile strength to well below 1 MPa, while the MCC-based tablets displayed a comparable or increasing tensile strength when comparing the tablets before and after microwave irradiation.

A greater variability in the disintegration time of the MDDS tablets was observed after microwave irradiation, ranging from approx. 12 sec to >30 min – the latter indicating incomplete disintegration in the investigated time frame and lying outside the Ph.Eur. specification for uncoated tablets (<15 min) (Table 1). Tablets based on large granules disintegrated significantly faster than tablets with small granules, irrespective of the filler. Generally, the MAN-based tablets displayed a more gradual increase in disintegration time with decreasing granule size and increasing compaction pressure, whereas tablets with MCC either disintegrated relatively fast or not at all (Table 1). At the lower microwave power input of 800 W, both tablets with MCC and MAN as the filler, disintegrated within 30 min, however, increasing disintegration times were observed predominantly for

tablets with small granules at higher compaction pressures (Table 1). At a power input of 1000 W during microwave irradiation, the MAN-based tablets displayed an increase in disintegration time with small granules, however, the tablets with large granules remained largely unaffected by the microwave irradiation and readily disintegrated. With MCC as the filler, neither tablets with small nor large granules achieved complete disintegration within 30 min at a 1000 W power input during microwave irradiation, correlating with the observed significant increase in tensile strength of these tablets and the fusion of granules indicated by the visual evaluation of the tablets (Table 1, Figure 2).

Table 1 Disintegration time and tensile strength of MDDS tablets prior to and after microwave irradiation (800 and 1000 W, 10 min). The most promising MDDS tablets with respect to a balance between their disintegration behaviour and tensile strength are marked in bold and grey. MW, microwaved. Mean +/- SD (tensile strength, n=10; disintegration time, n=6).

Formulation	Compaction pressure [MPa]	Tensile strength [MPa]			Disintegration time [min]		
		non-MW	800 W	1000W	non-MW	800 W	1000W
MCC large granules	100	0.8 ± 0.0	0.7± 0.3	2.1 ± 0.5	0.2 ± 0.0	0.2 ± 0.1	> 30
	150	1.3 ± 0.0	0.9 ± 0.2	2.3 ± 0.2	0.4 ± 0.0	0.5 ± 0.1	> 30
	200	**1.7 ± 0.1**	**1.3 ± 0.2**	**2.7 ± 0.6**	**2.1 ± 0.3**	**0.7 ± 0.2**	**> 30**
MCC small granules	**100**	**0.9 ± 0.1**	**1.1 ± 0.4**	**2.1 ± 0.7**	**0.3 ± 0.0**	**3.6 ± 2.2**	**> 30**
	150	1.4 ± 0.1	1.5 ± 0.4	2.6 ± 0.8	2.0 ± 0.4	20.1 ± 5.1	> 30
	200	1.7 ± 0.1	2.0 ± 0.5	3.7 ± 0.4	6.3 ± 0.8	> 30	> 30
MAN large granules	150	0.7 ± 0.0	0.4 ± 0.1	0.4 ± 0.1	1.0 ± 0.1	0.5 ± 0.0	0.5 ± 0.1
	200	1.1 ± 0.0	0.6 ± 0.1	0.6 ± 0.1	2.0 ± 0.2	0.7 ± 0.1	0.6 ± 0.1
	250	**1.3 ± 0.1**	**0.8 ± 0.1**	**0.6 ± 0.1**	**2.2 ± 0.3**	**5.8 ± 3.7**	**4.8 ± 4.5**
MAN small granules	**150**	**0.9 ± 0.0**	**0.7 ± 0.1**	**0.7 ± 0.1**	**3.1 ± 0.7**	**1.9 ± 1.7**	**2.7 ± 1.3**
	200	1.3 ± 0.0	1.0 ± 0.1	0.9 ± 0.1	5.2 ± 0.8	7.1 ± 4.4	20.2 ± 5.6
	250	1.5 ± 0.1	1.3 ± 0.1	1.3 ± 0.2	14.4 ± 1.6	15.6 ± 7.1	> 30

The significant decrease and increase in tensile strength for MCC- and MAN-based tablets before and after microwave irradiation, respectively, along with the observed positive correlation to the disintegration time could indicate potential physical changes within the entire tablets, and not only in the embedded granules, as a result of the *in situ* amorphisation process. Based on the results from sections 3.1 and 3.2, and in particular the disintegration behaviour after microwave irradiation (<15 min), four MDDS tablets (one for each of the fillers and granule sizes) were selected for further investigations (marked in bold in Table 1); MCC with large and small granules at a compaction pressure of 200 and 100 MPa, MAN with large and small granules at a compaction pressure of 250 and 150 MPa, respectively.

3.3 Internal tablet structure

To study the impact of microwave irradiation on the internal structure and to provide insights into the combined results of tensile strength and disintegration behaviour, the MDDS tablets were investigated by XµCT before and after microwave irradiation and the reconstructed cross-sections are displayed in Figure 3. Prior to microwave irradiation, the granules embedded in the filler matrix appeared visually intact, separated, and homogeneously distributed throughout the tablets, as indicated by the distinct high-density domains (white to light grey) in the cross-sections (Figure 3). Minor differences in the domains between the granules were distinguishable between the tablets, but this is thought to mainly relate to filler properties as well as the applied compaction pressure during manufacturing and affecting the porosity of the resulting tablets [57].

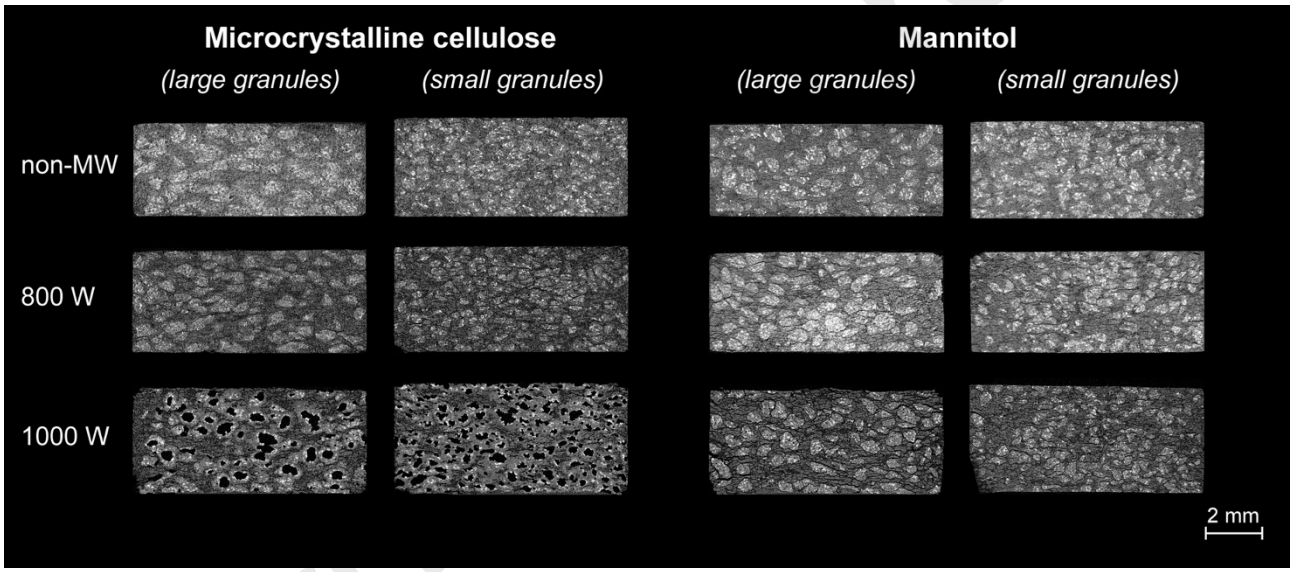

Figure 3 Reconstructed XµCT cross-sections of a selection of representative tablets (diameter = 8 mm) subject to microwave irradiation at 800 and 1000 W (10 min), as well as prior to microwave irradiation (non-MW). Tablets were prepared with different fillers, different granule particle sizes and different compaction pressures; i.e. microcrystalline cellulose with large and small granules at 200 and 100 MPa, and mannitol with large and small granules at 250 and 150 MPa, respectively. Scans at 6x6 um voxel size and a fixed scale. The greyscale, white to black, indicates high-to-low density.

After microwave irradiation at 800 and 1000 W, all the tablets displayed significant and visible changes in the internal structure (Figure 3). The embedded granules remained visually distinct and overall separated after microwave irradiation at 800 W, independent of the filler material and size of the granules. A decrease in density with additional horizontal fractures throughout the tablets and between granules was observed after microwave irradiation at 800 W, but the trend was more pronounced for the tablets with small granules and with MAN as filler compared to MCC-based tablets. Significant changes in the internal structures were

observed after microwave irradiation at 1000 W, where tablets with MCC displayed an increasing tendency to fracture as well as to form low-density pockets distributed throughout the tablet and across the tablet surface (Figure 3). The observed low-density pockets are suggested to be air-filled and arise from expanding water vapour during microwave irradiation at the increased power input as well as the ASD formation resulting from the fusion of individual drug and polymer particles within the granules. With the expansion of the granules in MCC at a power input of 1000 W during microwave irradiation, a true separation of the granules was not maintained, and fusion of granules was evident throughout the tablets and with both small as well as large granules. The MAN-based MDDS tablets displayed increased densification of the embedded granules at increasing microwave power input, but contrary to tablets with MCC, the granules remained separated by the filler material for both granule sizes at 1000 W. The tendency for primarily horizontal fracture seemed more pronounced for the MAN-based tablets with large granules and at a power input of 1000 W compared to small granules and a power input of 800 W (Figure 3).

The elucidated changes to the internal tablet structure correlate with the observed numerical change in tensile strength and disintegration time, as covered in section 3.2 (Table 1). The significant increase in tensile strength and associated lack of disintegration of MCC-based tables microwave irradiated at 1000 W can, therefore, be attributed to the fusion of granules throughout these tablets. Furthermore, the prevalent tendency to fracture observed for the microwave irradiated tablets based on MAN along with the separated granules can explain the observed significant decrease in tensile strength and the consistent disintegration behaviour.

3.4 Solid state of the ASD within the MDDS

The *in situ* ASD formation within the MDDS tablets and the dehydration of the NaH_2PO_4 monohydrate were investigated using XRPD and mDSC. Diffractograms of the microwave irradiated tablets were collected and selected representative MDDS tablets (section 3.2) covering both fillers, granule sizes, and microwave power inputs are displayed in Figure 4.

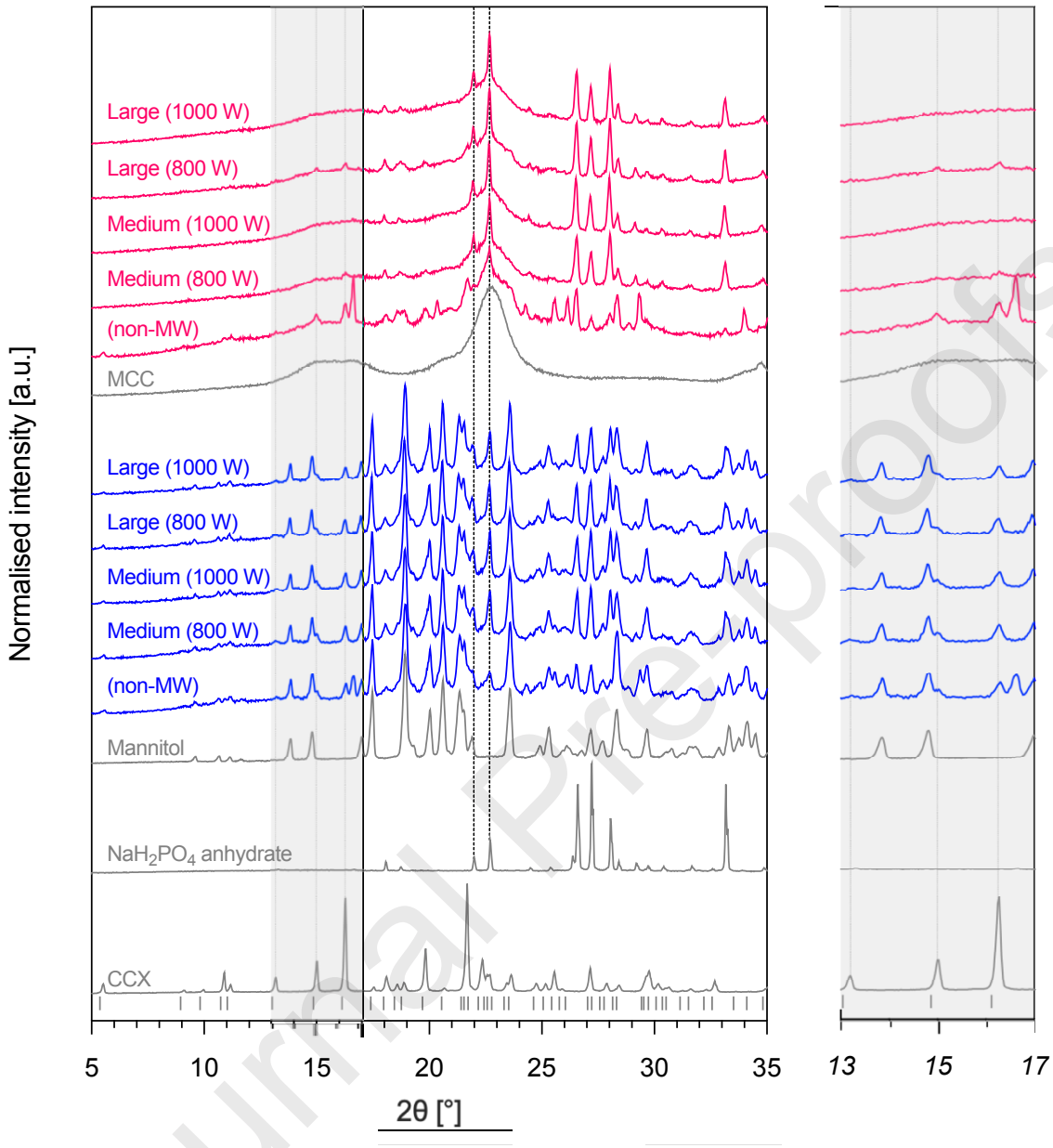

401

402 *Figure 4 X-ray powder diffractograms of selected MDDS tablets based on MCC (pink) and MAN (blue), as fillers and with*
403 *specified ASD granule sizes (large and small). The MDDS tablets were subjected to microwave radiation at 800 and 1000*
404 *W for 10 min. Tablets were prepared at the following compaction pressures: MCC large and small granules at 200 and 100*
405 *MPa, MAN large and small granules at 250 and 150 MPa, respectively. Diffractograms of bulk MCC, mannitol, NaH_2PO_4*
406 *anhydrate, and crystalline CCX are also shown to aid the reader. The most prominent Bragg peaks for CCX and NaH_2PO_4*
407 *anhydrate are marked with vertical lines. The position of Bragg peaks from the published crystal structure of CCX*
408 *(polymorphic form III) is indicated below the collected diffractogram [58, 59]. MW, microwaved.*

409 In common for all of the microwave irradiated MDDS tablets, the diffractograms were dominated by the signal
410 from the excipients used as fillers, with MCC displaying a broad bimodal diffraction signature, as a result of
411 the semi-crystalline nature of the material, and MAN showing sharp crystalline diffractions (Figure 4). Traces
412 of crystalline CCX (polymorphic form III [58, 59]) were visible at 13.2, 15.0, and 16.3 °2θ across all MAN-based

tablets, indicating incomplete *in situ* amorphisation (Figure 4). In addition, at a microwave power input of 800 W, MDDS tablets prepared with MCC as the filler resulted in incomplete amorphisation. However, complete amorphisation was achieved in the MCC-based tablets at a 1000 W power input with both small and large granules as evident by the absence of Bragg peaks corresponding to CCX (Figure 4).

In all investigated microwave irradiated tablets, Bragg peaks corresponding to NaH_2PO_4 anhydrate were visible at 22.0 and 22.7 °2θ, as a result of dehydration of the NaH_2PO_4 monohydrate (Figure 4). The observed dehydration indicates the release of water, which is necessary for dielectric heating as well as polymer plasticisation during microwave irradiation. The apparent residual CCX crystallinity in the MAN-based tablets may be explained by the observed delamination (Figure 3) and overall weakening of the tablets at increasing power inputs (Table 1) which, in turn, would decrease the amount of water retained in the tablets and being available for dielectric heating, ultimately affecting the *in situ* amorphisation process in a negative manner.

Further analysis of the microwave irradiated tablets by mDSC was conducted to confirm the presence of amorphous phases and residual crystalline material observed during XRPD analysis. The observed glass transition temperatures (T_gs), as well as the presence of melting endotherms, are reported in Table 2. One or more amorphous phases were present in all the investigated tablets after microwave irradiation, with the amorphous phase associated with the *in situ* prepared ASD of CCX and PVP/VA displaying comparable T_g's between 65.0 ± 0.1 and 77.5 ± 0.1 °C for all the investigated tablets. For the MCC-based tablets microwave irradiated with a power input of 800 W, a second T_g of approx. 121-124 °C was observed, indicating the presence of two amorphous phases in these two systems. The second glass transition can, however, be attributed to the amorphous fraction of the semi-crystalline filler, MCC [60]. Along with the presence of a second glass transition, a melting endotherm associated with residual crystalline CCX was also observed in the thermograms of the MCC tablets microwave irradiated at 800 W, confirming the incomplete amorphisation, also detected in the diffractograms (Table 2, Figure 4). For the comparable MCC-based tablets after microwave irradiation at 1000 W, neither a melting endotherm nor a second T_g were observed in the thermograms indicating complete amorphisation as well as the formation of homogenous ASDs.

As the melting point of neat MAN is approx. 165-167 °C [61, 62], it was difficult to separate the presence of residual crystalline CCX in the MAN-based tablets by mDSC due to the overlapping and depressed melting point of CCX (approx. 161-163 °C [59, 63]) in presence of the polymer [20].

Table 2 Thermal transitions observed during mDSC analysis of the selected MDDS tablets after microwave irradiation (800 and 1000 W, 10 min). Compaction pressure is indicated in parentheses; MCC large and small granules at 200 and 100 MPa, MAN large and small granules at 250 and 150 MPa, respectively. Mean +/- SD (n=3). [a] overlapping melting endotherms of CCX and MAN.

Formulation	MW power [W]	T_g^1 [°C]	T_g^2 [°C]	Melting endotherm
MCC, large (200 MPa)	800	76.1 ± 0.4	124.8 ± 4.2	Yes
large (200 MPa)	1000	77.5 ± 0.1	-	-
small (100 MPa)	800	76.1 ± 1.1	121.1 ± 0.1	Yes
small (100 MPa)	1000	76.6 ± 0.8	-	-
MAN, large (250 MPa)	800	65.0 ± 0.5	-	N/A [a]
large (250 MPa)	1000	72.2 ± 0.3	-	N/A [a]
small (150MPa)	800	71.2 ± 1.8	-	N/A [a]
small (150 MPa)	1000	71.7 ± 1.0	-	N/A [a]

3.5 Drug release behaviour

In order to evaluate the ability of the ASDs to create a supersaturated solution in the dissolution medium (FaSSIF), the drug release from the MDDS tablets was investigated in a non-sink *in vitro* dissolution configuration. Selected MDDS tablets were tested, including the completely amorphous MCC-based tablet with small granules, microwave irradiated at 1000 W, as well as the partially *in situ* amorphised MCC-based tablets microwaved at 800 W and MAN-based tablets microwaved at 1000 W. The dissolution profiles of the investigated tablets are displayed in Figure 5 and the derived dissolution parameters (maximum dissolution concentration, C_{max}, and apparent degree of supersaturation, aDS) are tabulated in Table 3. The tablets not subjected to microwave irradiation reached an apparent equilibrium solubility of approx. 42 µg/mL within 10 and 15 min independent of the choice of filler (MCC and MAN) (Figure 5). The observed apparent equilibrium

455 solubility of CCX in FaSSIF was in the range of previously reported literature solubilities (34-46 μg/mL) [64-
456 67].
457

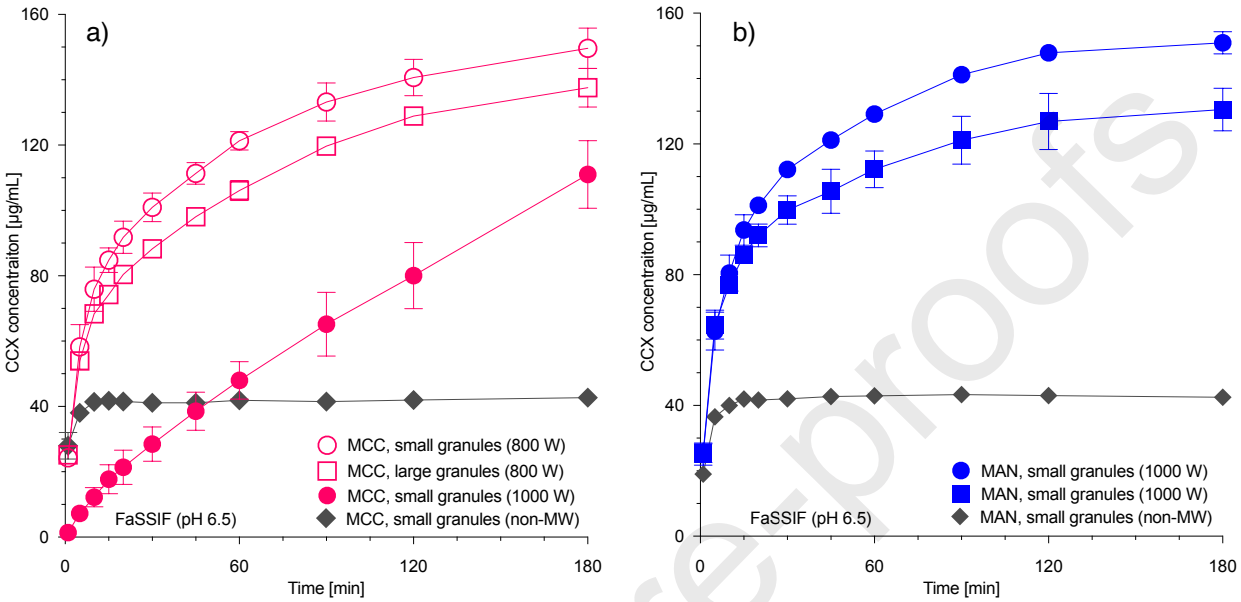

458

459 *Figure 5 Dissolution profiles of MDDS tablets based on a) MCC (pink), and, b) MAN (blue)) subject to microwave irradiation*
460 *for 10 min at 800 W (open symbols) and 1000 W (closed symbols) in FaSSIF (pH 6.5) at non-sink conditions for 0-3 h.*
461 *Granule size small (circle) and large (square). For reference, tablets with no exposure to microwave radiation (grey,*
462 *diamond) are included. Tablets were prepared with compaction pressures; MCC large and small granules at 200 and 100*
463 *MPa, MAN large and small granules at 250 and 150 MPa, respectively. MW, microwaved. Mean +/- SD (n=3).*

464 As seen in Figure 5, the *in situ* amorphised MDDS tablets were able to create a supersaturated CCX solution
465 in the dissolution medium in all of the investigated cases. However, differences in the rate of dissolution and
466 the degree of supersaturation are visible when comparing the dissolution profiles of tablets displaying
467 differences in the degree of drug amorphisation (partial/complete), disintegration behaviour (partial/complete),
468 filler type (MCC/MAN) as well as granule size (large/small). The dissolution profile of the completely *in situ*
469 amorphised MDDS tablets with small granules in MCC (microwave irradiated at 1000 W) displayed a close to
470 zero-order drug release with a lower initial drug release rate compared to the tablets prior to microwave
471 irradiation (Figure 5a, solid pink circles vs solid grey diamonds). This could be related to differences in the
472 disintegration behaviour, where the tablets prior to microwave irradiation displayed quick and complete
473 disintegration, whereas the *in situ* amorphised MDDS tablets were observed to only partially disintegrate during
474 dissolution. Nevertheless, supersaturation was achieved after >60 min, with a maximum dissolution
475 concentration (C_{max}) of 111 ± 1 μg/mL and an apparent degree of supersaturation (aDS) [68] of 2.6 (Table 3).

The partially *in situ* amorphised MDDS tablets displayed complete disintegration to individual granules and supersaturation of CCX was achieved within 5 min and sustained throughout the experimental time frame (3 h). Overall, a slightly higher initial drug release rate, C_{max}, and aDS were observed for microwave irradiated tablets with small granules compared to the large granules across both fillers (Figure 5, Table 3).

From a dissolution perspective, the most promising MDDS tablets with MCC and MAN achieved a C_{max} of 150 ± 6 and 151 ± 3 μg/mL, respectively, and were microwave irradiated tablets containing small granules (Figure 5). The achieved C_{max} corresponds to an aDS of approx. 3.5 for both formulations. For comparison, microwave irradiated tablets with large granules reached a C_{max} of 138 ± 6 μg/mL for MCC and 130 ± 7 μg/mL for MAN, corresponding to an aDS of 3.2 and 3.1, respectively (Table 3). The significantly reduced dissolution performance of the completely *in situ* amorphised MDDS tablets, compared to the partially amorphised, can be explained by the changes in the internal structure of the tablets, resulting in poor disintegration behaviour (Figure 3, Table 1). Hence, despite the complete amorphous nature of the embedded ASD as indicated by XRPD and mDSC (Figure 4, Table 2), it is paramount to develop an MDDS tablet with good disintegration of the dosage form to ensure a fast drug release from the ASD-based solid dosage forms.

Table 3 In vitro dissolution parameters derived at non-sink conditions in FaSSIF (Figure 5). aDS, apparent degree of supersaturation *[68]. Mean +/- SD (n=3).*

Formulation	MW power [W]	C_{max} [ug mL^{-1}]	aDS
MCC, large (200 MPa)	800	138 ± 6	3.2
small (100 MPa)	800	150 ± 6	3.5
small (100 MPa)	1000	111 ± 10	2.6
small (100 MPa)	-	43 ± 2	-
MAN, large (250 MPa)	1000	130 ± 7	3.1
small (150 MPa)	1000	151 ± 3	3.5
small (150 MPa)	-	43 ± 1	-

4. Conclusions

In this study, the suitability of the MDDS formulation concept for the preparation of supersaturated ASDs *in situ* by microwave irradiation was investigated. Here, the ASD-components (drug, polymer, dielectric excipient) were granulated together and subsequently incorporated in a tablet matrix of filler, disintegrant and lubricant. Both the granule size and the choice of filler, MCC and MAN, affected the tensile strength (0.7-1.7 MPa) and

disintegration time (<15 min) before microwave irradiation. All tablets retained the initial cylindrical form during and after microwave irradiation (800 and 1000 W), however, the tensile strength and disintegration time were found to increase with increasing power input, in particular for MCC-based tablets. Moreover, the 1000 W power input during microwave irradiation coincided with complete *in situ* amorphisation of the CCX in the MCC-based tablets, while the investigated MDDS tablet formulations displayed partial amorphisation. XμCT suggested a fusion of otherwise separated granules as the cause for the observed increase in tensile strength, which in turn resulted in a lack of disintegration in the experimental timeframe (>30 min) for the fully amorphised MCC-based tablets. On the other hand, the partially amorphised MDDS tablets disintegrated, which was reflected in their *in vitro* dissolution performance, where a supersaturation was observed already within 5 min and reaching a maximum supersaturation of approx. 3.5-fold during the experiments. The poor disintegration behaviour of the otherwise fully *in situ* amorphised MDDS tablets significantly impacted the overall dissolution performance, despite the amorphous nature of the embedded ASD granules. As a result, the dissolution rate was decreased and supersaturation was only observed after 60 min. In principle, the study showed that the MDDS tablet concept allowed microwave-induced *in situ* amorphisation of supersaturated ASDs in individual granules, while simultaneously maintaining the structural and geometric integrity of the tablets and improving the disintegration and dissolution performance. However, the MDDS concept could see further improvement in both disintegration and *in situ* amorphisation performance.

5. Acknowledgements

This work was supported by the Independent Research Fund Denmark [grant number DFF-7026-00052B].

6. Declaration of interest

The authors declare no conflict of interest.

6. References

[1] T.N. Hiew, D.Y. Zemlyanov, L.S. Taylor, Balancing Solid-State Stability and Dissolution Performance of Lumefantrine Amorphous Solid Dispersions: The Role of Polymer Choice and Drug–Polymer Interactions, Mol. Pharm. 19 (2022) 392-413.

[2] T. Takagi, C. Ramachandran, M. Bermejo, S. Yamashita, L.X. Yu, G.L. Amidon, A Provisional Biopharmaceutical Classification of the Top 200 Oral Drug Products in the United States, Great Britain, Spain, and Japan, Mol. Pharm. 3 (2006) 631-643.

[3] C.A. Lipinski, Drug-like properties and the causes of poor solubility and poor permeability, J. Pharmacol. Toxicol. Methods. 44 (2000) 235-249.

[4] N.J. Babu, A. Nangia, Solubility Advantage of Amorphous Drugs and Pharmaceutical Cocrystals, Cryst. Growth. Des. 11 (2011) 2662-2679.

[5] L.S. Taylor, G.G.Z. Zhang, Physical chemistry of supersaturated solutions and implications for oral absorption, Adv. Drug Del. Rev. 101 (2016) 122-142.

[6] H. Grohganz, K. Löbmann, P. Priemel, K. Tarp Jensen, K. Graeser, C. Strachan, T. Rades, Amorphous drugs and dosage forms, J. Drug Deliv. Sci. Technol. 23 (2013) 403-408.

[7] K.S. Ingersoll, J. Cohen, The impact of medication regimen factors on adherence to chronic treatment: a review of literature, J. Behav. Med. 31 (2008) 213-224.

[8] A. Singh, Z.A. Worku, G. Van den Mooter, Oral formulation strategies to improve solubility of poorly water-soluble drugs, Expert Opin. Drug Deliv. 8 (2011) 1361-1378.

[9] H.D. Williams, N.L. Trevaskis, S.A. Charman, R.M. Shanker, W.N. Charman, C.W. Pouton, C.J. Porter, Strategies to address low drug solubility in discovery and development, Pharmacol. Rev. 65 (2013) 315-499.

[10] B.C. Hancock, M. Parks, What is the true solubility advantage for amorphous pharmaceuticals?, Pharm. Res. 17 (2000) 397-404.

[11] B.C. Hancock, G. Zografi, Characteristics and significance of the amorphous state in pharmaceutical systems, J. Pharm. Sci. 86 (1997) 1-12.

[12] E.O. Kissi, H. Grohganz, K. Löbmann, M.T. Ruggiero, J.A. Zeitler, T. Rades, Glass-transition temperature of the β-relaxation as the major predictive parameter for recrystallization of neat amorphous drugs, J. Phys. Chem. B 122 (2018) 2803-2808.

[13] L.R. Hilden, K.R. Morris, Physics of amorphous solids, J. Pharm. Sci. 93 (2004) 3-12.

[14] T. Vasconcelos, S. Marques, J. das Neves, B. Sarmento, Amorphous solid dispersions: Rational selection of a manufacturing process, Adv. Drug Del. Rev. 100 (2016) 85-101.

[15] G. Van den Mooter, The use of amorphous solid dispersions: A formulation strategy to overcome poor solubility and dissolution rate, Drug Discov. Today Technol. 9 (2012) 79-85.

[16] S. Baghel, H. Cathcart, N.J. O'Reilly, Polymeric Amorphous Solid Dispersions: A Review of Amorphization, Crystallization, Stabilization, Solid-State Characterization, and Aqueous Solubilization of Biopharmaceutical Classification System Class II Drugs, J. Pharm. Sci. 105 (2016) 2527-2544.

[17] C. Bhugra, M.J. Pikal, Role of thermodynamic, molecular, and kinetic factors in crystallization from the amorphous state, J. Pharm. Sci. 97 (2008) 1329-1349.

[18] Y. Tian, J. Booth, E. Meehan, D.S. Jones, S. Li, G.P. Andrews, Construction of drug-polymer thermodynamic phase diagrams using Flory-Huggins interaction theory: identifying the relevance of

559 temperature and drug weight fraction to phase separation within solid dispersions, Mol. Pharm. 10 (2013)
560 236-248.

561 [19] S.V. Jermain, C. Brough, R.O. Williams, 3rd, Amorphous solid dispersions and nanocrystal technologies
562 for poorly water-soluble drug delivery - An update, Int. J. Pharm. 535 (2018) 379-392.

563 [20] M.M. Knopp, L. Tajber, Y. Tian, N.E. Olesen, D.S. Jones, A. Kozyra, K. Löbmann, K. Paluch, C.M.
564 Brennan, R. Holm, A.M. Healy, G.P. Andrews, T. Rades, Comparative Study of Different Methods for the
565 Prediction of Drug–Polymer Solubility, Mol. Pharm. 12 (2015) 3408-3419.

566 [21] S.V. Bhujbal, B. Mitra, U. Jain, Y. Gong, A. Agrawal, S. Karki, L.S. Taylor, S. Kumar, Q. Zhou,
567 Pharmaceutical amorphous solid dispersion: A review of manufacturing strategies, Acta Pharm. Sin. B. 11
568 (2021) 2505-2536.

569 [22] P. Tran, Y.-C. Pyo, D.-H. Kim, S.-E. Lee, J.-K. Kim, J.-S. Park, Overview of the Manufacturing Methods
570 of Solid Dispersion Technology for Improving the Solubility of Poorly Water-Soluble Drugs and Application to
571 Anticancer Drugs, Pharmaceutics 11 (2019) 1-26.

572 [23] B. Démuth, Z.K. Nagy, A. Balogh, T. Vigh, G. Marosi, G. Verreck, I. Van Assche, M.E. Brewster,
573 Downstream processing of polymer-based amorphous solid dispersions to generate tablet formulations, Int.
574 J. Pharm. 486 (2015) 268-286.

575 [24] A. Sauer, S. Warashina, S.M. Mishra, I. Lesser, K. Kirchhöfer, Downstream processing of spray-dried
576 ASD with hypromellose acetate succinate – Roller compaction and subsequent compression into high ASD
577 load tablets, Int. J. Pharm.: X. 3 (2021) 100099.

578 [25] A. Otte, Y. Zhang, M.T. Carvajal, R. Pinal, Milling induces disorder in crystalline griseofulvin and order in
579 its amorphous counterpart, CrystEngComm 14 (2012) 2560-2570.

580 [26] K.r. Bērziņš, S.J. Fraser-Miller, T. Rades, K.C. Gordon, Low-Frequency Raman Spectroscopic Study on
581 Compression-Induced Destabilization in Melt-Quenched Amorphous Celecoxib, Mol. Pharm. 16 (2019) 3678-
582 3686.

583 [27] Z. Ayenew, A. Paudel, G. Van den Mooter, Can compression induce demixing in amorphous solid
584 dispersions? A case study of naproxen–PVP K25, Eur. J. Pharm. Biopharm. 81 (2012) 207-213.

585 [28] R.S. Dhumal, S.L. Shimpi, A.R. Paradkar, Development of spray-dried co-precipitate of amorphous
586 celecoxib containing storage and compression stabilizers, Acta. Pharm. 57 (2007) 287-300.

587 [29] N.K. Thakral, S. Mohapatra, G.A. Stephenson, R. Suryanarayanan, Compression-induced crystallization
588 of amorphous indomethacin in tablets: characterization of spatial heterogeneity by two-dimensional X-ray
589 diffractometry, Mol. Pharm. 12 (2015) 253-263.

590 [30] P.A. Priemel, H. Grohganz, T. Rades, Unintended and in situ amorphisation of pharmaceuticals, Adv.
591 Drug Del. Rev. 100 (2016) 126-132.

592 [31] M. Doreth, M.A. Hussein, P.A. Priemel, H. Grohganz, R. Holm, H. Lopez de Diego, T. Rades, K.
593 Lobmann, Amorphization within the tablet: Using microwave irradiation to form a glass solution in situ, Int. J.
594 Pharm. 519 (2017) 343-351.

[32] W. Qiang, K. Löbmann, C.P. McCoy, G.P. Andrews, M. Zhao, Microwave-Induced In Situ Amorphization: A New Strategy for Tackling the Stability Issue of Amorphous Solid Dispersions, Pharmaceutics 12 (2020) 1-19.

[33] M. Doreth, K. Lobmann, P. Priemel, H. Grohganz, R. Taylor, R. Holm, H. Lopez de Diego, T. Rades, Influence of PVP molecular weight on the microwave assisted in situ amorphization of indomethacin, Eur. J. Pharm. Biopharm. 122 (2018) 62-69.

[34] M. Edinger, M.M. Knopp, H. Kerdoncuff, J. Rantanen, T. Rades, K. Lobmann, Quantification of microwave-induced amorphization of celecoxib in PVP tablets using transmission Raman spectroscopy, Eur. J. Pharm. Sci. 117 (2018) 62-67.

[35] N. Hempel, M. Knopp, R. Berthelsen, J. Zeitler, K. Löbmann, The influence of drug and polymer particle size on the in situ amorphization using microwave irradiation, Eur. J. Pharm. Biopharm. 149 (2020) 77-84.

[36] R.R. Mishra, A.K. Sharma, Microwave–material interaction phenomena: Heating mechanisms, challenges and opportunities in material processing, Compos. Part A Appl. Sci. Manuf. 81 (2016) 78-97.

[37] M. Vollmer, Physics of the microwave oven, Phys. Educ. 39 (2003) 74-81.

[38] P. Bergese, I. Colombo, D. Gervasoni, L.E. Depero, Microwave generated nanocomposites for making insoluble drugs soluble, Mater. Sci. Eng., C 23 (2003) 791-795.

[39] T. Wong, Use of Microwave in Processing of Drug Delivery Systems, Curr. Drug Del. 5 (2008) 77-84.

[40] U. Kaatze, The dielectric properties of water in its different states of interaction, J. Solution Chem. 26 (1997) 1049-1112.

[41] P. Lunkenheimer, S. Emmert, R. Gulich, M. Köhler, M. Wolf, M. Schwab, A. Loidl, Electromagnetic-radiation absorption by water, Phys. Rev. E. 96 (2017) 062607.

[42] M.B. Rask, M.M. Knopp, N.E. Olesen, R. Holm, T. Rades, Influence of PVP/VA copolymer composition on drug–polymer solubility, Eur. J. Pharm. Sci. 85 (2016) 10-17.

[43] N.-J. Hempel, M.M. Knopp, J.A. Zeitler, R. Berthelsen, K. Löbmann, Microwave-Induced in Situ Drug Amorphization Using a Mixture of Polyethylene Glycol and Polyvinylpyrrolidone, J. Pharm. Sci. 110 (2021) 3221-3229.

[44] T.P. Holm, M.M. Knopp, K. Löbmann, R. Berthelsen, Microwave induced in situ amorphisation facilitated by crystalline hydrates, Eur. J. Pharm. Sci. (2021) 105858.

[45] T.P. Holm, M.M. Knopp, R. Berthelsen, K. Löbmann, Supersaturated amorphous solid dispersions of celecoxib prepared *in situ* by microwave irradiation, Int. J. Pharm. (2022) 122115.

[46] W. Qiang, K. Löbmann, M. Manne Knopp, C. P. McCoy, G. P. Andrews, M. Zhao, Investigation into the role of the polymer in enhancing microwave-induced in situ amorphization, Int. J. Pharm. (2021) 121157.

[47] A.R. Rajabi-Siahboomi, Overview of Multiparticulate Systems for Oral Drug Delivery, in: A.R. Rajabi-Siahboomi (Ed.) Multiparticulate Drug Delivery: Formulation, Processing and Manufacturing, Springer New York, New York, NY, 2017, pp. 1-4.

[48] J.T. Fell, J.M. Newton, Determination of Tablet Strength by the Diametral-Compression Test, J. Pharm. Sci. 59 (1970) 688-691.

[49] A. Fedorov, R. Beichel, J. Kalpathy-Cramer, J. Finet, J.-C. Fillion-Robin, S. Pujol, C. Bauer, D. Jennings, F. Fennessy, M. Sonka, J. Buatti, S. Aylward, J.V. Miller, S. Pieper, R. Kikinis, 3D Slicer as an image computing platform for the Quantitative Imaging Network, Magn. Reson. Imaging 30 (2012) 1323-1341.

[50] L. Tive, Celecoxib clinical profile, Rheumatology 39 (2000) 21-28.

[51] D. Clemett, K.L. Goa, Celecoxib, Drugs 59 (2000) 957-980.

[52] G.S. Geis, Update on clinical developments with celecoxib, a new specific COX-2 inhibitor: What can we expect?, Scand. J. Rheumatol. 28 (1999) 31-37.

[53] R. Berthelsen, E. Sjögren, J. Jacobsen, J. Kristensen, R. Holm, B. Abrahamsson, A. Müllertz, Combining in vitro and in silico methods for better prediction of surfactant effects on the absorption of poorly water soluble drugs—a fenofibrate case example, Int. J. Pharm. 473 (2014) 356-365.

[54] C. Schiller, C.P. Fröhlich, T. Giessmann, W. Siegmund, H. Mönnikes, N. Hosten, W. Weitschies, Intestinal fluid volumes and transit of dosage forms as assessed by magnetic resonance imaging, Aliment. Pharmacol. Ther. 22 (2005) 971-979.

[55] M. Leane, K. Pitt, G. Reynolds, A proposal for a drug product Manufacturing Classification System (MCS) for oral solid dosage forms, Pharm. Dev. Technol. 20 (2015) 12-21.

[56] N. Tarlier, I. Soulairol, N. Sanchez-Ballester, G. Baylac, A. Aubert, P. Lefevre, B. Bataille, T. Sharkawi, Deformation behavior of crystallized mannitol during compression using a rotary tablet press simulator, Int. J. Pharm. 547 (2018) 142-149.

[57] A.K. Schomberg, A. Diener, I. Wünsch, J.H. Finke, A. Kwade, The use of X-ray microtomography to investigate the microstructure of pharmaceutical tablets: Potentials and comparison to common physical methods, Int. J. Pharm.: X. 3 (2021) 100090.

[58] R. Vasu Dev, K. Shashi Rekha, K. Vyas, S.B. Mohanti, P. Rajender Kumar, G. Om Reddy, Celecoxib, a COX-II inhibitor, Acta Crystallogr. C Struct. Chem. 55 (1999).

[59] G.W. Lu, M. Hawley, M. Smith, B.M. Geiger, W. Pfund, Characterization of a novel polymorphic form of celecoxib, J. Pharm. Sci. 95 (2006) 305-317.

[60] L. Szcześniak, A. Rachocki, J. Tritt-Goc, Glass transition temperature and thermal decomposition of cellulose powder, Cellulose 15 (2008) 445-451.

[61] Á. Gombás, P. Szabó-Révész, G. Regdon, I. Erős, Study of thermal behaviour of sugar alcohols, J. Therm. Anal. Calorim. 73 (2003) 615-621.

661 [62] A. Burger, J.-O. Henck, S. Hetz, J.M. Rollinger, A.A. Weissnicht, H. Stöttner, Energy/Temperature
662 Diagram and Compression Behavior of the Polymorphs of d-Mannitol, J. Pharm. Sci. 89 (2000) 457-468.

663 [63] A.R. Paradkar, B. Chauhan, S. Yamamura, A.P. Pawar, Preparation and Characterization of Glassy
664 Celecoxib, Drug Dev. Ind. Pharm. 29 (2003) 739-744.

665 [64] M.M. Knopp, J.H. Nguyen, C. Becker, N.M. Francke, E.B. Jorgensen, P. Holm, R. Holm, H. Mu, T.
666 Rades, P. Langguth, Influence of polymer molecular weight on in vitro dissolution behavior and in vivo
667 performance of celecoxib:PVP amorphous solid dispersions, Eur. J. Pharm. Biopharm. 101 (2016) 145-151.

668 [65] M.M. Knopp, J.H. Nguyen, H. Mu, P. Langguth, T. Rades, R. Holm, Influence of Copolymer Composition
669 on In Vitro and In Vivo Performance of Celecoxib-PVP/VA Amorphous Solid Dispersions, AAPS J. 18 (2016)
670 416-423.

671 [66] M. Arndt, H. Chokshi, K. Tang, N.J. Parrott, C. Reppas, J.B. Dressman, Dissolution media simulating the
672 proximal canine gastrointestinal tract in the fasted state, Eur. J. Pharm. Biopharm. 84 (2013) 633-641.

673 [67] Y. Shono, E. Jantratid, N. Janssen, F. Kesisoglou, Y. Mao, M. Vertzoni, C. Reppas, J.B. Dressman,
674 Prediction of food effects on the absorption of celecoxib based on biorelevant dissolution testing coupled
675 with physiologically based pharmacokinetic modeling, Eur. J. Pharm. Biopharm. 73 (2009) 107-114.

676 [68] L.I. Blaabjerg, H. Grohganz, E. Lindenberg, K. Löbmann, A. Müllertz, T. Rades, The Influence of
677 Polymers on the Supersaturation Potential of Poor and Good Glass Formers, Pharmaceutics 10 (2018) 164.

678

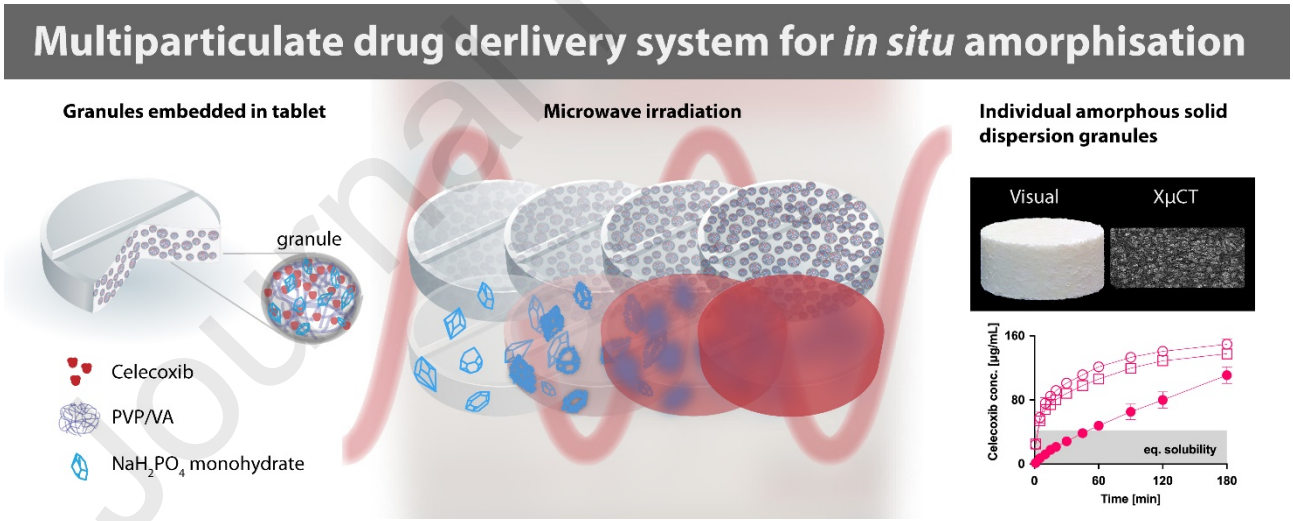

679